

## Midlatitude particle and electric field effects at the onset of the November 1993 geomagnetic storm

J. C. Foster

Haystack Observatory, Massachusetts Institute of Technology, Westford

S. Cummer and U. S. Inan

STAR Lab, Stanford University, Stanford, California

**Abstract.** Millstone Hill incoherent scatter radar elevation scans across midlatitudes captured the ionospheric response to storm-induced electric field and precipitation-induced changes near the equatorward extent of the expanding auroral region during the early phases of the November 3–4, 1993, magnetic storm. Solar wind-induced magnetospheric compression was observed at ~2307 UT [Borovsky *et al.*, this issue] and a prompt, short-duration (10 min) increase in the upward plasma velocity to > 100 m/s at ~2319 UT on November 3, 1993 signaled the onset of the storm-induced enhancement of the eastward electric field over Millstone Hill in the premidnight sector at 54° invariant latitude ( $\Lambda$ ). This resulted in an uplifting of the *F* region ionosphere above the site by ~80 km by 2330 UT. Formation of a narrow ionospheric trough poleward of the Millstone site accompanied the auroral convection enhancement at somewhat later times while plasmashet precipitation produced the ionization at altitudes between 200 and 300 km at  $\Lambda < 60^\circ$  observed by the radar. Strong precipitation of energetic particles from the outer radiation belt was observed by SAMPEX at 58.5°  $\Lambda$ , near the equatorward limit of the plasmashet precipitation observed by DMSP and Millstone Hill. Amplitude perturbations of VLF signals propagating in the Earth-ionosphere waveguide serve to localize the energetic radiation belt precipitation to latitudes between 56°  $\Lambda$  and 58.5°  $\Lambda$  and provide accurate timing of storm-induced energetic precipitation, whose onset was at ~2332 UT in the premidnight sector. A later enhancement of the eastward electric field at latitudes equatorward of Millstone Hill and the storm-induced trough led to a perturbation of the midlatitude ionosphere to  $\Lambda < 40^\circ$  and is the subject of a companion paper [Foster and Rich, this issue].

### 1. Introduction

During geomagnetic disturbances, the electric fields and particle populations that characterize the auroral region expand equatorward and their effects are felt at previously sub-auroral latitudes [e.g. Yeh *et al.*, 1991; Foster, 1995]. The equatorward extent of the plasma sheet particle population lies on field lines near the plasma-pause and precipitation from the plasma sheet alters the ionospheric conductances, currents and fields. These, combined with the time-dependent effects of injected particles, serve to shield the inner magnetosphere from the strong auroral disturbances. During such conditions, an intense polarization electric field can be set up near the equatorward extent of the pre-midnight sunward convection and this drives the latitudinally narrow polarization jet or sub-auroral ion drifts (SAID) [Galperin *et al.*, 1974; Spiro *et al.*, 1979]. Associated with the region of strongest convection, frictional heating leads to atmospheric chemistry changes and a deep, narrow *F* region trough is formed [Schunk *et al.*, 1976]. Energetic electrons at higher *L* values in the outer radiation belt are lost as their gradient-drift paths intersect newly opened field lines on the dayside, while strong precipitation mechanisms lead to radiation belt dumping and *D* region ionization in the night sector at lower *L* values in the auroral region. The dynamic coupling between the magnetosphere

and ionosphere at previously subauroral latitudes is especially pronounced during the expansion of auroral phenomena and the growth and decay of electric-field shielding which accompany the early phases of impulsive magnetic disturbances. Here we use a variety of space-based and ground-based sensors to detail the chronology, spatial extent, and synchronism of the phenomena observed near  $L=3.5$  (58° invariant latitude  $\Lambda$ ) during the early phases of the November 3–4, 1993, event.

### 2. Observations and Discussion

The November 3–4, 1993, storm event was characterized by a sudden and severe response of the magnetosphere and ionosphere to a strong solar wind perturbation. Details of the event and the solar wind driver are found in the work of Foster and Rich [this issue] and the other papers devoted to this event in this issue. As a contribution to the overall understanding of this event, this paper focuses on the relative timing and spatial location of effects observed at magnetic mid latitudes in the pre-midnight sector during storm onset. We find electric fields to provide a prompt signature of the storm intensification and an electric field-induced uplifting of the *F* layer peak height was the first observed midlatitude effect. This was followed 10 min later by the onset of VLF propagation perturbations which indicate the onset of the energetic precipitation in this local time sector. We find the latitude extent of outer zone energetic precipitation to coincide with the extent of VLF propagation perturbations and collocate the precipitation bands

Copyright 1998 by the American Geophysical Union.

Paper number 98JA00018.  
0148-0227/98/98JA-00018\$09.00

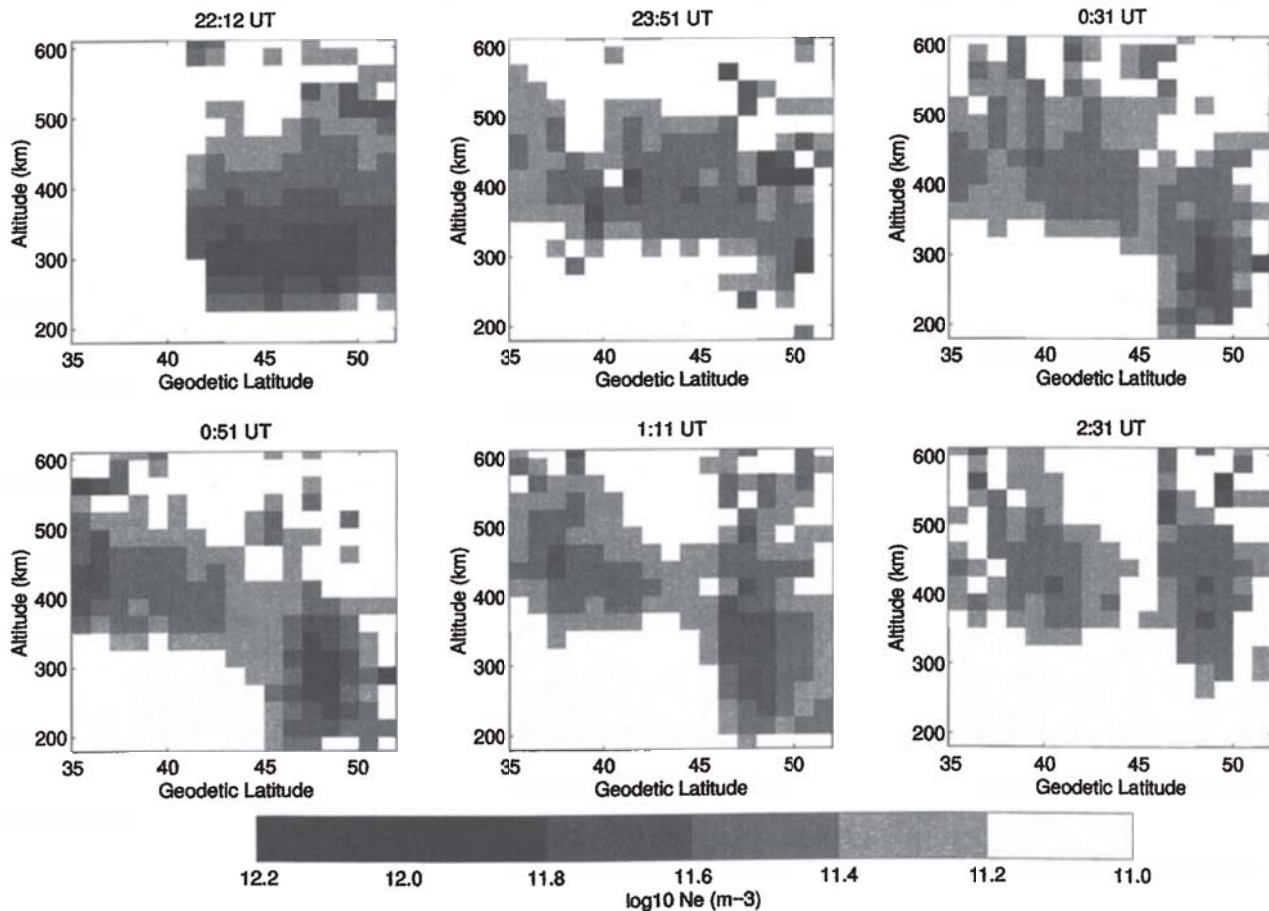


**Figure 1.** Elevation scans with the Millstone Hill incoherent scatter radar depict the evolution of the latitude-altitude structure of the ionospheric *F*-region density during the onset of the geomagnetic storm on November 3-4, 1993. Precipitation-produced ionization is evident near 48° latitude beginning with the scan near 2351 UT, and a pronounced ionization trough is formed during the event near 45°.

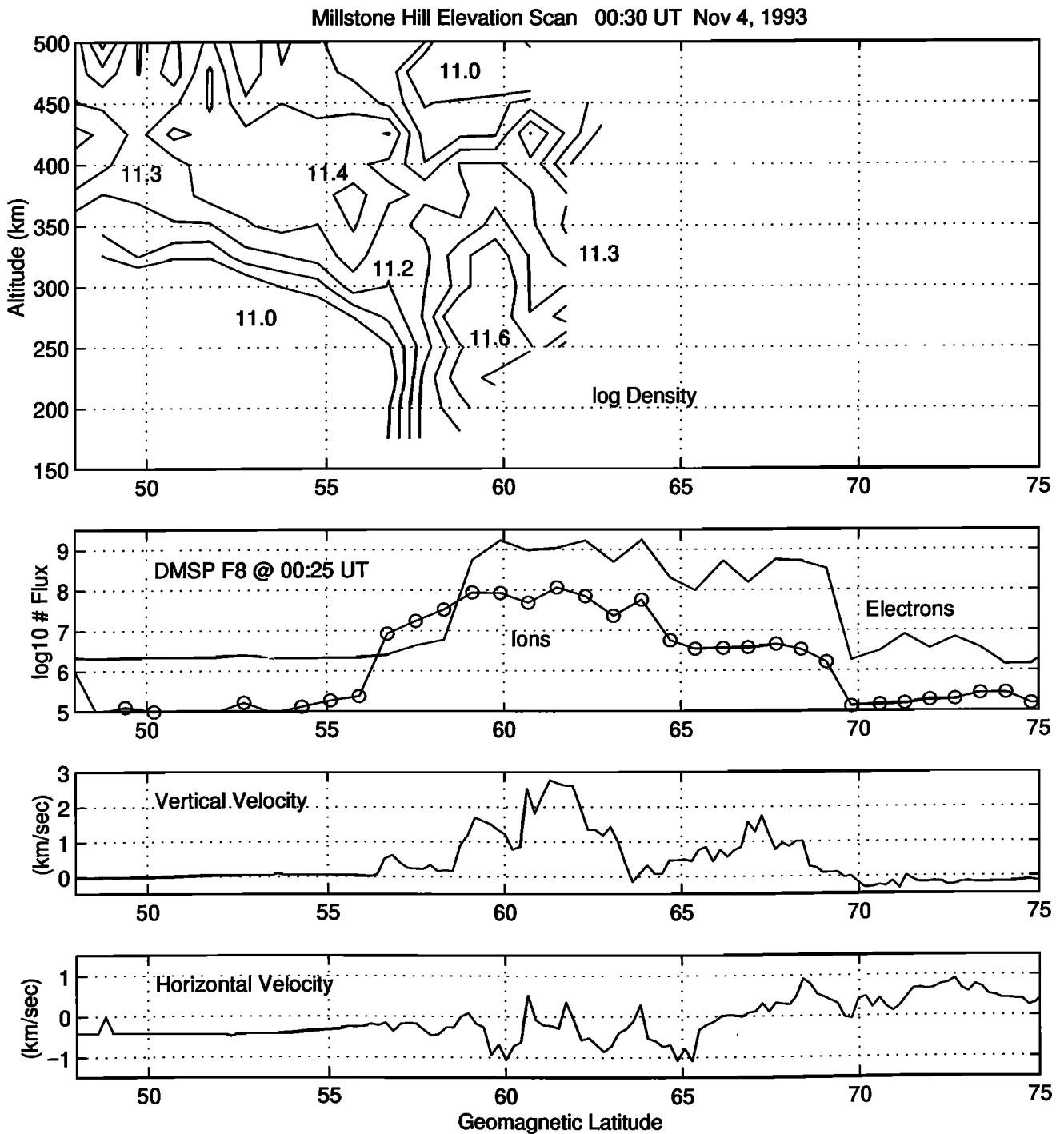
at the poleward edge of the depleted outer zone with the inner edge of storm-enhanced plasma sheet electrons.

A radar/radiotomography campaign, the Russian-American Tomography Experiment (RATE), was being conducted during the early phases of the severe geomagnetic disturbance on November 3-4, 1993. Elevation scans were performed with the Millstone Hill incoherent scatter radar and these provided observations of ionospheric plasma concentration (density), temperatures, and line-of-sight velocity over a 180 - 500 km altitude range and over the magnetic latitude range 49°Λ to 67°Λ with 20-min time resolution. Radar and tomographic observations were made through the interval beginning immediately preceding the storm onset and continuing through the subsequent period of rapid ionospheric trough formation and the enhancement of lower *F* region ionization at mid latitudes caused by low-energy particle precipitation. A description of the RATE campaign and the intercomparisons of the radar and radiotomography observations through the initial phases of the November 3-4, 1993, storm are reported by Foster *et al.* [1994b] and a further description of the event and the mid- and low-latitude effects of a penetrating eastward electric field near 0030 UT on November 4, 1993, are presented by Foster and Rich [this issue].

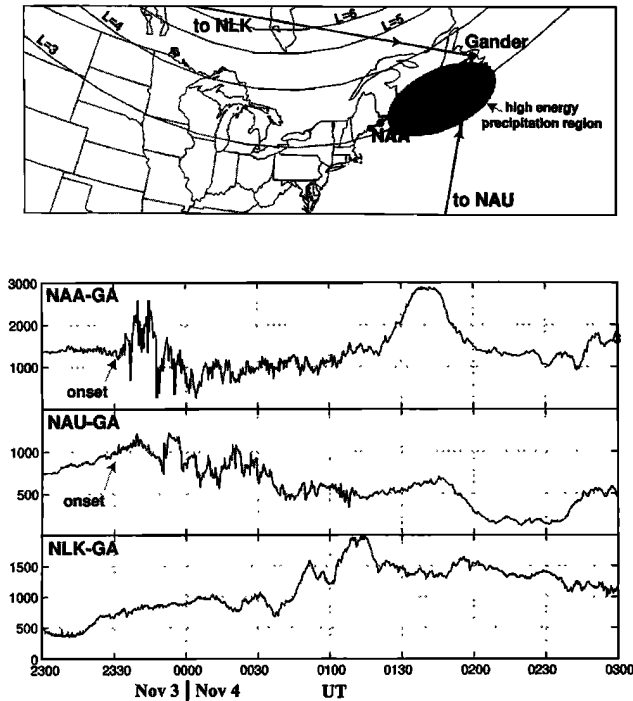
### 2.1. Millstone Hill Incoherent Scatter Radar

Figure 1 presents a set of six Millstone Hill radar elevation scans which are representative of the effects observed by the radar during the event. Scans are presented in geodetic latitude; invariant latitude

= geodetic latitude + 12° on the Millstone Hill meridian. Radio-frequency interference and spike-like system noise persisted through the experiment and these result in the random, small-scale pseudodensity enhancements most apparent at altitudes > 500 km. Each panel presents temperature-corrected, calibrated electron density versus latitude and altitude observed during a single scan of the antenna from north to south. Radar scans were taken with a 20-min scan repetition time while zenith altitude profiles above Millstone Hill were taken every 10 minutes throughout the experiment. The panel at 2212 UT on November 3 shows the conditions before the main disturbance onset. Borovsky *et al.* [this issue] report magnetopause compression to inside geosynchronous orbit at ~2307 UT. (Local midnight at Millstone Hill occurs at 0500 UT, and storm onset occurred when the meridian of the radar observations was at 1800 MLT.) A rather uniform *F* layer is seen with peak altitude, *hmF2*, near 280 km. By 2351 UT, the rapidly growing disturbance produced a pronounced uplifting of the sub-auroral *F* layer (*hmF2* ~ 400 km) which we attribute to the effects of an eastward electric field at storm onset. Such an eastward electric field [cf. Buonsanto and Foster, 1993] can penetrate to latitudes well equatorward of the ionospheric trough and into the region where the effects of horizontal plasma transport due to the convection electric field become negligible [cf. Yeh *et al.*, 1991]. The effects of developing particle precipitation in the expanding auroral region are seen near 49° latitude as an ionization enhancement at *F* region heights below 300 km. High electron temperatures in this region and spatial coinci-



**Figure 2.** Intercomparison of nearly-simultaneous, colocated observations of the *F* region with the radar (top panel) and plasmashet particles and ion drift with the DMSP F-8 satellite (lower panels). DMSP integrated particle number flux ( $\# \text{ cm}^{-2} \text{ sec}^{-1} \text{ sr}^{-1}$ ) for electrons (line) and ions (o) between 30 eV and 30 keV is presented in the 2nd panel. The inner edge of the plasmashet electrons ( $\sim 58.5^\circ \Lambda$ ) is colocated with the *F* region (200 km - 300 km altitude) density enhancement seen by the radar (top panel) and is coincident with the position of the precipitation band at the poleward extent of the storm-depleted outer radiation belt (cf. Figure 4). The DMSP upward vertical drift velocity exceeds the  $2.7 \text{ km s}^{-1}$  instrument saturation near  $62^\circ$  in response to the very intense ion and electron precipitation.



**Figure 3.** VLF propagation paths from North American transmitters to Gander, Newfoundland (GA) serve to localize the latitude extent of energetic particle precipitation (see text). VLF amplitude perturbations (lower panels, presented in relative receiver units) began at  $\sim 2332$  UT and were confined to the propagation paths below  $L=3.5$ , indicating that the  $>100$  keV electron precipitation was confined to magnetic latitudes  $< 58^\circ\Lambda$  in the pre-midnight sector.

dence with the low-latitude edge of the the electron plasma sheet, discussed below, indicate a particle-precipitation source for this ionization enhancement. At 0031 UT on November 4, a sharply defined trough is apparent near  $45^\circ$  latitude and strong precipitation-enhanced density is seen poleward of  $46^\circ$  and extending at least to  $51^\circ$ . The radar field of view limits observations of the ionization enhancement to altitudes  $> 180$  km. Comparison with a radiotomographic reconstruction of the ionospheric density obtained during an overflight of a Russian navigation satellite coincident with this scan [Foster *et al.*, 1994b] confirmed that the radar signal enhancement in this region corresponded to a real increase in the lower  $F$  region plasma density, and was not produced by coherent backscatter accompanying increased convection electric field strength poleward of the radar [cf. Foster *et al.*, 1992]. The most distinctive radar signature of the developing activity was a brief (20 min) uplifting of the  $F$  region plasma equatorward of the trough observed during the 0031 UT scan, such that the peak altitude increased with distance equatorward from the trough. This phenomenon is not treated in detail in this paper, but Foster and Rich [this issue] discuss the evidence for a penetrating eastward electric field at 0030 UT on November 4 which produced this further uplifting of the  $F$  layer and an array of ionospheric phenomena at latitudes equatorward of the trough.

The precipitation signature poleward of the trough continued to intensify until after 0111 UT, and then diminished, leaving the well-

defined trough around  $45^\circ$  geodetic latitude ( $\sim 57^\circ\Lambda$ ). The tomographic reconstructions of Bust *et al.* [1997] depict a narrow ( $< 2^\circ$ ) midlatitude trough near  $53^\circ\Lambda$  near 0400 UT at a central-U.S. longitude. The RATE tomographic/radar experiments [Foster *et al.*, 1994b] found the narrow ( $< 2^\circ$ ) trough at  $285^\circ$  E longitude to be at  $53^\circ\Lambda$  at 0456 UT. In the absence of an  $F$  region ionization source, a nighttime density depletion, such as the storm-produced midlatitude trough, will remain well-defined even after the trough-formation mechanisms have ceased to operate [Evans *et al.*, 1983]. Such fossil troughs corotate with the earth and stay nearly fixed in the radar field of view until they are erased by the solar-produced ionization at dawn. We suggest that the narrow trough observed later in the event by Foster *et al.* [1994b] and Bust *et al.* [1997] was formed during storm onset within the field of view of the Millstone Hill radar, as depicted in Figure 1.

## 2.2. DMSP F8 Satellite Overflight

Observations of particle precipitation and plasma drifts made as the DMSP F8 satellite overflew the region sampled by the radar scans provide a context for the interpretation of the midlatitude effects associated with storm onset. Particle flux and drift meter velocities are compared with the nearly coincident 00:31 UT scan radar scan in Figure 2 (here displayed in magnetic coordinates to facilitate comparison with the DMSP data). Electron precipitation seen by DMSP extended poleward from  $58.5^\circ$  magnetic latitude, coincident with the region of the radar ionization enhancement below 300 km altitude. An upward ion velocity in excess of  $2.5$  km  $s^{-1}$  was observed at  $61^\circ$  associated with the expansion of the topside ionosphere in the region of the strong auroral heating. Ion fluxes extended some  $2^\circ$  equatorward of the electrons, spanning the trough latitudes. This is the characteristic particle signature across the region of a subauroral ion drifts (SAID), whose strong convection can be responsible for trough formation. Strong horizontal velocity was not seen in this region at the time of the overflight, although a velocity  $> 2500$  m/s, consistent with a SAID, was seen at this latitude somewhat earlier by DMSP F10 (not shown). Anderson *et al.* [1991] discuss evidence for the existence of fossil SAID, regions of residual enhanced sunward convection related to prior SAID intensifications. Foster *et al.* [1994a] relate the deep storm-enhanced ionospheric trough to the location of active and fossil SAID and a co-located stable auroral red (SAR) arc. Because of nearly full-moon conditions on the night of November 3-4, no optical observations were obtained from Millstone Hill which could confirm the occurrence of a SAR arc during this event, although the radar observed electron temperatures enhanced by a factor of 3 to  $> 4000^\circ$  K at 400-km altitude within the trough.

## 2.3. VLF Propagation Perturbation

Electromagnetic waves at VLF frequencies are strongly reflected by the ground and  $D$  region of the ionosphere, which form the Earth-ionosphere waveguide. Any changes in the phase and amplitude of these narrowband signals correspond to variations in the  $D$  region, which occur on a variety of timescales, ranging from 10 to 100 s for localized electron density enhancements caused by lightning-induced electron precipitation [Inan and Carpenter, 1987], to 1 hour for the large-scale changes caused by the appearance of high-energy ( $>100$  keV) auroral electron precipitation over the propagation path [Cummer *et al.*, 1997].

Continuous observations of the amplitude and phase of sub-ionospheric-propagating VLF signals from navigation and communication transmitters were made in Gander, Newfoundland in 1993 and 1994. Figure 3 shows a map of the great-circle propa-

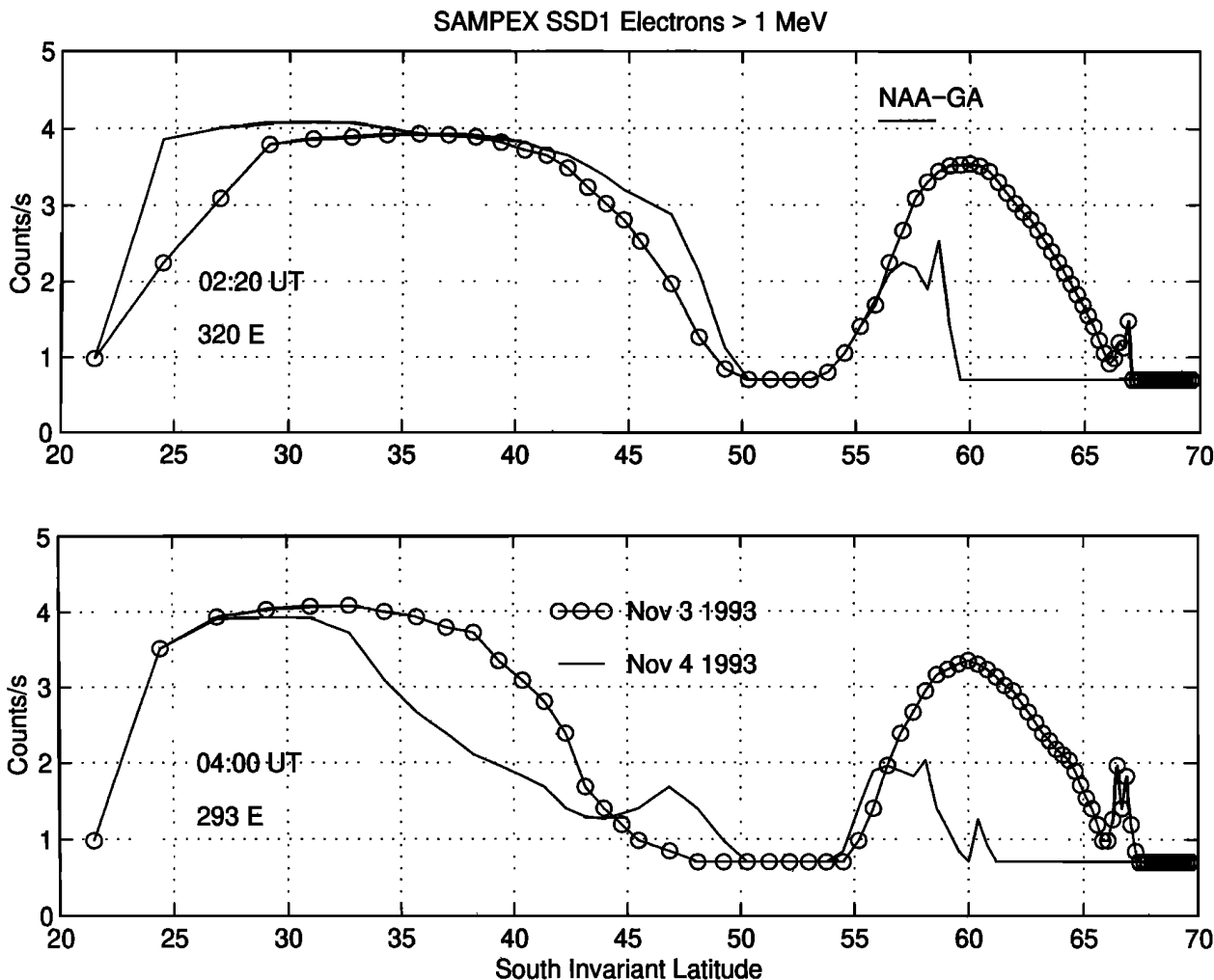


**Figure 4.** Significant changes occurred in the inner and outer radiation belts during the early phases of the November 4, 1993, event (see text). SAMPEX observations of  $> 1$  MeV electron count rate for particles mirroring below 600 km altitude are shown for directly comparable passes on November 3 (o) and 4. A precipitation band has been identified by Nakamura *et al.* [1995] at  $58.5^\circ\Lambda$  at 0220 UT and the outer radiation zone is depleted poleward of this latitude [Li *et al.*, 1997]. The latitude extent of the perturbed NAA-GA VLF propagation path is indicated.

gation paths from three different transmitters to Gander, as well as the footprint of the  $L$  shells in this region. At the bottom of Figure 3 are presented the amplitudes of the signals from these three transmitters received at Gander over a 4-hour period on November 3-4. At 2332 UT on November 3, a sudden and dramatic increase in the variability of the signal along NAA (Cutler, Maine)-GA (Gander) propagation path begins. (This path is the shortest of the three and therefore the most sensitive to ionospheric changes.) A similar change occurs simultaneously on the much longer NAU (Agadilla, Puerto Rico)-GA path to the east. The northern NLK (Jim Creek, Washington)-GA path shows no such fast oscillations. The oscillations on these two propagation paths endure until approximately 0100 UT on November 4, after which they appear to decay slowly and end by 0130 UT.

These data indicate that the ionospheric  $D$  region began to change at 2332 UT and that this change was not steady but rather showed great temporal variability (possibly in multiple locations) because of the oscillatory nature of the VLF amplitude perturbations. Occurrence of such an ionospheric disturbance at  $D$  region altitudes implies significant particle precipitation at energies

greater than  $\sim 100$  keV in order to cause the observed ionospheric changes below  $\sim 80$  km. Comparison with Figure 2 indicates that the high-energy precipitation was confined to the most equatorward portion of the 0.3 - 30 keV precipitation seen by DMSP F8.

We can also conclude from the configuration of the paths that this precipitation was limited to latitudes equatorward of  $58^\circ\Lambda$  ( $L < 3.5$ ) because the NLK-GA path (which is everywhere north of the receiver at Gander except very close to the transmitter) did not exhibit any precipitation effects. The precipitation region must have also been somewhat distributed in longitude in order to appear on both the NAA and NAU paths, but the extent is uncertain because the latitude cannot be precisely determined. We indicate by shading in Figure 3 that portion of the propagation paths which were effected by precipitation.

It is in principle possible to interpret the VLF perturbations quantitatively, in the context of a VLF propagation model [Poulsen *et al.*, 1993] and models of ionospheric density enhancements produced by precipitating electrons [Glukhov *et al.*, 1992]. Such analyses have been used to study the characteristics of ionospheric regions heated by HF heaters [Bell *et al.*, 1995] and the effects of auroral

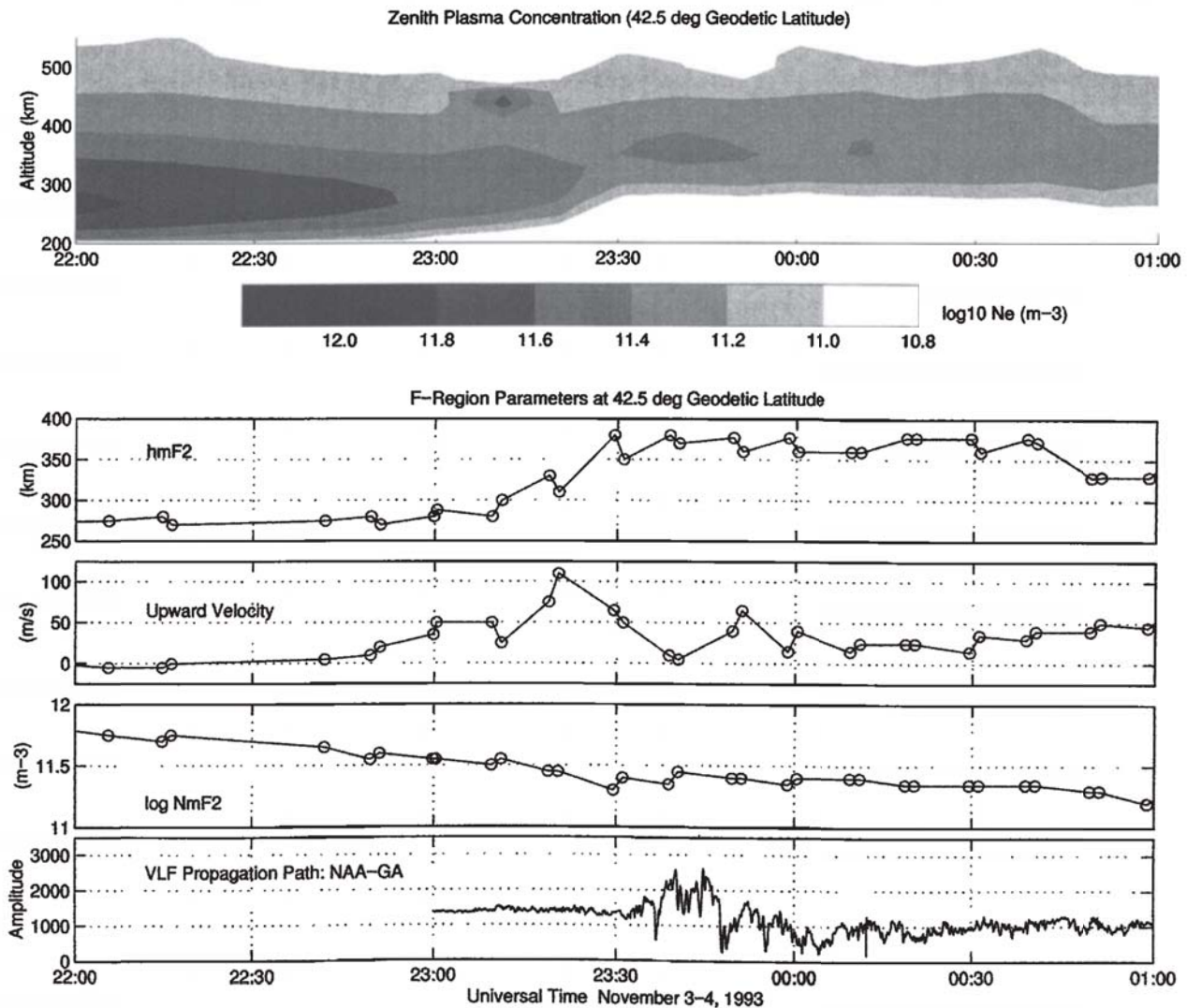


**Figure 5.** Combined radar and VLF propagation (lower panel) data summarize the timing of the subauroral latitude electric field and particle precipitation effects during the November 3-4, 1993, storm onset. Zenith-antenna Ne/altitude profiles (top panel) indicate a rapid uplifting of the F layer peak altitude (hmF2) shortly before 2330 UT. Upward directed ion velocity (middle panel) increased sharply at 2319 UT, providing the first observation of subauroral latitude electric field effects. VLF amplitude perturbations began at 2332 UT (lower panel), indicating the onset of >1 MeV electron precipitation near the Millstone Hill longitude.

particle precipitation on the D region [Cummer *et al.*, 1997]. However, such an analysis is beyond the scope of this paper, especially in view of the fact that multiple ionospheric disturbances, each highly variable in time, were likely involved.

#### 2.4. Outer Zone Energetic Particle Precipitation

Relativistic precipitation from the radiation belts can result in a large energy deposition rate at altitudes between 40 and 80 km [Baker *et al.*, 1987], resulting in the perturbation of the VLF signal transmission characteristics across the effected region. Li *et al.* [1997] describe the SAMPEX instruments and observations and provide a detailed account of the changes in the outer zone ( $L > 3$ ) relativistic electrons during this event. Figure 4 presents SAMPEX southern-hemisphere nighttime data from the SSD1 instrument, which is sensitive to energetic electrons with energy > 1 MeV, for passes across the latitudes of interest for November 3 and 4, 1993.

The SAMPEX satellite is in a near-circular orbit near 600 km and samples the high-energy radiation belt particles mirroring at/or below that altitude. Particle fluxes observed are highly longitude dependent, but passes at the same universal time (longitude) are highly repeatable from day to day in the absence of perturbing disturbances that effect the radiation belt environment. Passes from two longitudes near Millstone Hill and the South Atlantic magnetic anomaly (SAA) are shown during the early hours of the disturbance onset on November 4. Observations along these longitudes from the preceding day are shown for comparison and to aid in identifying the storm-induced effects. Precipitation bands [Nakamura *et al.*, 1995] are seen at 0220 UT on Nov 4th at  $58.5^\circ \Lambda$  [Li *et al.*, 1997], at the poleward edge of the residual outer zone electron fluxes. The outer zone has been depleted (presumably by precipitation) across the  $56^\circ \Lambda - 58.5^\circ \Lambda$  extent of the perturbed NAA-GA VLF propagation path whose extent (in the conjugate hemisphere) is indicated on the figure. The SAMPEX data are consistent with the relationship

between VLF perturbation and energetic precipitation described by *Cummer et al.* [1997] and with our interpretation of the VLF propagation perturbation presented in the preceding section. The magnetic field is weak in the vicinity of the SAA, lowering the mirror heights of energetic particles in its vicinity and resulting in stronger precipitating fluxes in the southern hemisphere than in the northern conjugate region where the radar and VLF propagation perturbations were observed. The preceding SAMPEX pass at 0045 UT (345° E longitude; not shown) also located the precipitation band near 58°  $\Lambda$ . The earliest observation of a significant depletion of the outer radiation zone during the event was made on a pass over the European sector (10° E longitude; not shown) at 2315 UT which found a precipitation band at  $L=4.25$  (61°  $\Lambda$ ), indicating energetic precipitation at a somewhat higher latitude at that earlier time.

In addition to the nearly complete loss of the outer zone energetic particles poleward of 58.5°  $\Lambda$  ( $L=3.7$ ) during this storm, discussed by *Li et al.* [1997], there are marked changes in the inner zone radiation belt structure. Increased electron fluxes seen near 47°  $\Lambda$  ( $L=2.15$ ) indicate the formation of a new inner radiation belt in the gap between the normal inner and outer zones during this event. Enhancements of the inner zone fluxes at the SAMPEX altitude are seen near 26.5°  $\Lambda$  ( $L=1.23$ ) at longitudes near the peak of the SAA during the 0220 UT pass on November 4. Somewhat to the west of the SAA, flux reductions spanning the range 26.5°  $\Lambda$  to 42°  $\Lambda$  ( $L=1.23 - L=1.8$ ) are seen during the 0400 UT pass. Coincidentally,  $L=1.23$  marks the position of the strong low/mid latitude ionospheric perturbation, also associated with the SAA, reported by *Foster and Rich* [this issue]. The SAMPEX observations reported above indicate that the > 1 MeV particles of the inner radiation belt were perturbed in that vicinity. Enhanced precipitation and losses from the inner zone near the SAA during the storm can set up a charge-separation electric field across the SAA which enhances the local eastward electric field and provides a possible mechanism for the destabilization of the low and mid-latitude ionosphere during such storm events (e.g. *Foster and Rich* [this issue]).

### 2.5. Event Timing

Figure 5 summarizes the timing of the sub-auroral-latitude electric field and particle precipitation effects during the November 3-4, 1993, storm onset. Zenith-antenna Millstone Hill radar observations were taken every 10 min through the event and these reveal a sharp increase in the upward plasma velocity near 2320 UT. The peak upward velocity  $\sim 100$  m/s is consistent with a transient, eastward electric field of  $\sim 15$  mV/m. The electric field provides a prompt signature of the major storm intensification and, within the 10-min sampling uncertainty of the radar experiment, provides the first midlatitude signature of the storm-related effects. The increase in the upward velocity was short lived, indicating an  $\sim 15$  min lifetime for the eastward electric field enhancement. The observed height of the  $F$  layer peak responded to this electric field-induced uplifting and rose to  $\sim 360$  km by 2330 UT and remained at this elevated altitude for several hours.  $F$  layer balance-height calculations [*Buonsanto et al.*, 1989] indicate the occurrence of an equatorward neutral wind after 2330 UT, with magnitude  $\sim 100$  m s<sup>-1</sup> at 0000 UT and increasing steadily to  $\sim 250$  m s<sup>-1</sup> by 0100 UT on November 4. This storm-induced equatorward surge maintained the  $F$  layer peak altitude near 350 km after the initial uplift by the electric field. The density at the  $F$  peak,  $NmF2$ , continued its post-sunset decrease through this interval, without any sharp or strong perturbation. The VLF propagation-perturbation data provide an accurate timing for the onset of the energetic precipitation in the premidnight sector during the event and the NAA-GA VLF amplitude-perturbation

data are presented in the lowest panel. These indicate the onset of the energetic outer zone precipitation in the premidnight sector to have begun near 2332 UT.

*Bust et al.* [1997] report midlatitude ionosonde virtual height observations from the central United States and find no evidence of an increase in the height of the  $F$  layer until after 0200 UT on November 4, 1993. While it is possible that the  $F$  layer uplifting seen in the Millstone Hill data at  $\sim 2330$  UT on November 3, 1993 (cf. Figure 5) was confined to the shielding region near the Millstone latitude and did not extend equatorward to the latitude of the ionosonde reported by *Bust et al.* [1997], the penetrating uplifting reported by *Foster and Rich* [this issue] extended far equatorward of Millstone Hill. The fact that this was not observed at the central-US longitude by *Bust et al.* [1997] reinforces the conclusion of *Foster and Rich* [this issue] that the later enhancement of the eastward electric field effect in the inner magnetosphere was narrowly confined in longitude.

### 3. Summary

We have used a variety of space-based and ground-based sensors to detail the chronology and synchronism of the phenomena observed during the early phases of the November 1993 geomagnetic storm. The ionospheric effects of electric fields observed by the Millstone Hill radar provide a prompt response to the storm intensification and the first subauroral latitude signature of the storm-related effects at  $\sim 2320$  UT on November 3. Comparison of the latitudinal distribution of  $F$  region density observed by the radar with particle-precipitation data seen during a DMSP F8 overflight, indicates that a narrow storm-induced trough formed at the equatorward edge of the auroral precipitation, in the region where the ions extended equatorward of the plasmashet electron population. VLF propagation data indicate the onset of the energetic outer zone precipitation in the premidnight sector to occur at 2332 UT. A comparison of the VLF propagation and the DMSP particle data indicates that the high-energy precipitation was confined to the most equatorward portion of the 0.3 - 30 keV precipitation seen by DMSP, and was coincident with the latitude of relativistic precipitation bands observed by SAMPEX which were associated with the loss of the outer-zone energetic electron population during the event.

Our study has shown the following:

1. An uplifting of the  $F$  layer by an eastward electric field is the first storm-related phenomenon observed at subauroral latitudes in the evening sector.
2. Energetic electron precipitation delineating the poleward edge of the outer radiation zone occurs near the equatorward limit of plasma sheet electrons in this local time sector.
3. The spatial extent of VLF propagation perturbations coincides with the region of precipitation losses from the outer zone.
4. VLF amplitude perturbations provide a precise means of timing energetic particle precipitation events on field lines intersecting the propagation path.

**Acknowledgments.** A portion of this work was conducted while J. Foster was a Visiting Professor at the Solar-Terrestrial Environment Laboratory of Nagoya University. The contributions of F. Rich in providing and interpreting the DMSP observations are gratefully acknowledged as are helpful discussions with R. Nakamura, M. Buonsanto, and members of the Atmospheric Sciences Group at the MIT Haystack Observatory. The SAMPEX data of Figure 4 were provided by R. Nakamura and D. N. Baker. Millstone Hill observations and analysis are supported by the National Science Foun-

dition through a cooperative agreement with the Massachusetts Institute of Technology. The VLF work at Stanford University was funded by the Air Force Office of Scientific Research under grant F19628-96-C-0149.

The Editor thanks A. S. Rodger for his assistance in evaluating this paper.

## References

- Anderson, P. C., R. A. Heelis, and W. B. Hanson, The ionospheric signatures of rapid sub-auroral ion drifts, *J. Geophys. Res.*, **96**, 5785-5792, 1991.
- Baker, D. N., J. B. Blake, D. J. Gorney, P. R. Higbie, R. W. Klebesadel, and J. H. King, Highly relativistic magnetospheric electrons: A role in coupling to the middle atmosphere, *Geophys. Res. Lett.*, **14**, 127-1030, 1987.
- Bell, T. F., U. S. Inan, M. T. Danielson, and S. A. Cummer, VLF signatures of ionospheric heating by HIPAS, *Radio Sci.*, **30**, 1855-1867, 1995.
- Borovsky, J., M. F. Thomsen, D. J. McComas, T. E. Cayton, and D. J. Knipp, Magnetospheric dynamics and mass flow during the November 1993 storm, *J. Geophys. Res.*, this issue.
- Buonsanto, M. J., and J. C. Foster, Effects of magnetospheric electric fields and neutral winds on the low-latitude ionosphere during the March 20-21, 1990 storm, *J. Geophys. Res.*, **98**, 19133-19140, 1993.
- Buonsanto, M. J., J. E. Salah, K. L. Miller, W. L. Oliver, R. G. Burnside, and P. G. Richards, Observations of neutral circulation at mid-latitudes during the Equinox Transition Study, *J. Geophys. Res.*, **94**, 16987-16997, 1989.
- Bust, G. S., T. L. Gaussiran II, and D. S. Coco, Ionospheric observations of the November 1993 storm, *J. Geophys. Res.*, **102**, 14293-14304, 1997.
- Cummer, S. A., T. F. Bell, U. S. Inan, and D. L. Chenette, VLF remote sensing of high-energy auroral particle precipitation, *J. Geophys. Res.*, **102**, 7477-7484, 1997.
- Evans, J. V., J. M. Holt, W. L. Oliver, and R. H. Wand, The fossil theory of nighttime high latitude *F* region troughs, *J. Geophys. Res.*, **88**, 7769-7782, 1983.
- Foster, J. C., Radar Observations of magnetosphere-ionosphere coupling at mid and high latitudes, *J. Geomagn. Geoelect.*, **47**, 801-812, 1995.
- Foster, J. C., and F. J. Rich, Prompt mid-latitude electric field effects during severe geomagnetic storms, *J. Geophys. Res.*, this issue.
- Foster, J. C., D. Tetenbaum, C. F. del Pozo, J. -P. St. Maurice, and D. R. Moorcroft, Aspect angle variations in intensity, phase velocity, and altitude for high-latitude 34-cm *E* region irregularities, *J. Geophys. Res.*, **97**, 8601-8617, 1992.
- Foster, J. C., M. J. Buonsanto, M. Mendillo, D. Nottingham, F. J. Rich, and W. Denig, Coordinated stable auroral red arc observations: Relationship to plasma convection, *J. Geophys. Res.*, **99**, 11,429-11,439, 1994a.
- Foster, J. C., M. J. Buonsanto, J. M. Holt, J. A. Klobuchar, P. Fougere, W. Pakula, T. D. Raymond, V. E. Kumitsyn, E. S. Andreeva, E. D. Tereshchenko, and B. Z. Khudukon, Russian-American Tomography Experiment, *Int. J. Imag. Sys. Tech.*, **5**, 148-159, 1994b.
- Galperin, Y., V. N. Ponomarev, and A. G. Zosimova, Plasma convection in the polar ionosphere, *Ann. Geophys.*, **30**, 1-7, 1974.
- Glukhov, V. S., V. P. Pasko, and U. S. Inan, Relaxation of transient lower ionospheric disturbances caused by lightning-whistler-induced electron precipitation bursts, *J. Geophys. Res.*, **97**, 16971-16979, 1992.
- Inan, U. S., and D. L. Carpenter, Lightning-induced electron precipitation events observed at  $L \sim 2.4$  as phase and amplitude perturbations on subionospheric VLF signals, *J. Geophys. Res.*, **92**, 3293-3303, 1987.
- Li, X., D. N. Baker, M. Temerin, T. E. Cayton, E. G. D. Reeves, R. A. Christensen, J. B. Blake, M. D. Looper, R. Nakamura, and S. G. Kanekal, Multisatellite observations of the outer zone electron variation during the November 3-4, 1993, magnetic storm, *J. Geophys. Res.*, **102**, 14123-14140, 1997.
- Nakamura, R., D. N. Baker, J. B. Blake, S. Kanekal, B. Klecker, and D. Hovestadt, Relativistic electron precipitation enhancements near the outer edge of the radiation belt, *Geophys. Res. Lett.*, **22**, 1129-1132, 1995.
- Poulsen, W. L., U. S. Inan, and T. F. Bell, A multiple-mode three-dimensional model of VLF propagation in the Earth-ionosphere waveguide in the presence of localized *D* region disturbances, *J. Geophys. Res.*, **98**, 1705-1717, 1993.
- Schunk, R. W., P. M. Banks, and W. J. Raitt, Effects of electric fields and other processes upon the nighttime high-latitude *F* layer, *J. Geophys. Res.*, **80**, 3271-3282, 1976.
- Spiro, R. W., R. A. Heelis, and W. B. Hanson, Rapid sub-auroral ion drifts observed by Atmospheric Explorer C, *Geophys. Res. Lett.*, **6**, 657-660, 1979.
- Yeh, H.-C., J. C. Foster, F. J. Rich, and W. Swider, Storm-time electric field penetration observed at mid-latitude, *J. Geophys. Res.*, **96**, 5707-5721, 1991.

S. Cummer and U. S. Inan, STAR Laboratory, Stanford University, 321 Durand Building, Stanford, CA 94305. (e-mail: cummer@nova.stanford.edu; inan@sierra.stanford.edu)

J. C. Foster, Haystack Observatory, Massachusetts Institute of Technology, Route 40, Westford, MA 01886-1299. (e-mail: jcf@hydra.haystack.edu)

(Received August 6, 1997; revised December 23, 1997; accepted December 29, 1997.)